Scaling rates of true polar wander in convecting planets and moons

Journal:	*Geophysical Journal International*
Manuscript ID	GJI-S-16-0216
Manuscript Type:	Research Paper
Date Submitted by the Author:	15-Mar-2016
Complete List of Authors:	Rose, Ian; UC Berkeley, Earth and Planetary Science Buffett, Bruce; University of California Berkeley, Earth and Planetary Science
Keywords:	Earth rotation variations < GEODESY and GRAVITY, Palaeomagnetism < GEOMAGNETISM and ELECTROMAGNETISM, Numerical solutions < GEOPHYSICAL METHODS, Dynamics: convection currents, and mantle plumes < TECTONOPHYSICS, Mantle processes < GENERAL SUBJECTS, Planetary interiors < PLANETS

submitted to *Geophys. J. Int.*

Scaling rates of true polar wander in convecting planets and moons

Ian Rose[1] and Bruce A. Buffett[1]

[1] *Department of Earth & Planetary Science, University of California, Berkeley, CA 94720, USA. E-mail: ian.rose@berkeley.edu*

SUMMARY

Mass redistribution in the convecting mantle of a planet can cause perturbations in its moment of inertia tensor. Conservation of angular momentum dictates that these perturbations can change the direction of the rotation vector of the planet, a process known as true polar wander (TPW). Although the existence of TPW on Earth is well-verified, its rate and magnitude over geologic time scales remain controversial. Here we present scaling analyses and numerical simulations of TPW due to mantle convection over a range of parameter space relevant to planetary interiors. For simple rotating convection, the most important parameters are the Rayleigh number, the rotation rate, and the size of relative density fluctuations (i.e. thermal expansivity times the temperature variations). We identify timescales for the growth of moment of inertia perturbations due to convection and for their relaxation due to true polar wander. These timescales, as well as the relative sizes of convective anomalies, control the rate and magnitude of TPW. This analysis also clarifies the nature of so called "inertial interchange" TPW events, and when they are likely to occur. Finally, we discuss implications for large-scale TPW in Earth's past, which has been suggested to be important for life and climate history.

Key words: Earth rotation variations; Mantle processes; Dynamics: convection currents and mantle plumes; Planetary interiors; Numerical solutions; Paleomagnetism applied to tectonics.

1 INTRODUCTION

A rotating, quasistatic body like a planetary mantle will tend to spin about the axis of its maximum moment of inertia. Convection in a planetary mantle continuously redistributes mass, which can change the moment of inertia tensor, necessitating a change in the spin axis of the planet to conserve angular momentum, a process known as true polar wander (TPW).

TPW was first considered in detail by Darwin (1887), and the theory has been subsequently developed by many (e.g. Munk & MacDonald 1960; Goldreich & Toomre 1969; Ricard et al. 1993). Despite this, the ability of internal mass anomalies to drive large-scale TPW remains controversial. Paleomagnetic data have been interpreted to require up to $3^\circ - 12^\circ$/Myr rates of TPW (Mitchell et al. 2011), but the ability of the mantle to respond at such rates has been questioned (Tsai & Stevenson 2007).

The primary uncertainties in assigning a maximum TPW rate to a convecting planet are the size of convective anomalies, which drive the rotational adjustment, and the viscosity structure of the mantle, which retards it. These two uncertainties are not unrelated: they are both expected to be functions of the geometric and material properties of the mantle. As such, they do not vary independently, and first-order questions about the propensity for planets to experience TPW remain: how are rates of TPW expected to vary with the vigor of convection? Are other planetary bodies more or less likely than Earth to experience TPW? And are these rates expected to vary in Earth history?

These questions suggest that an approach rooted in dimensional analysis and fluid dynamics can clarify the rates and magnitudes of TPW. Most previous studies coupling mantle convection models to polar wander calculations have done so with prescribed density perturbations (e.g. Greff-Lefftz 2004), or prescribed moment of inertia variations (e.g. Tsai & Stevenson 2007; Creveling et al. 2012). Richards et al. (1999) coupled thermal convection models to a polar wander model, but did not address in detail the scaling relationships between the two.

Herein we perform a scaling analysis of rates of TPW for a minimal system of a rotating, convecting mantle, which we support with numerical simulations.

2 ROTATIONAL DYNAMICS

2.1 The Liouville equation

Conservation of angular momentum for a torque-free system in a rotating reference frame requires

$$\frac{d\mathbf{H}}{dt} + \mathbf{\Omega} \times \mathbf{H} = 0 \tag{1}$$

where $\mathbf{H} = \mathbf{I} \cdot \mathbf{\Omega}$ is the angular momentum vector, $\mathbf{I}$ is the moment of inertia tensor, and $\mathbf{\Omega}$ is the angular velocity vector. On a dynamic planet $\mathbf{I}$ may be a function of time, so to conserve angular momentum $\mathbf{\Omega}$ must be also vary with time. In this case Equation (1) is often called the Liouville equation (e.g. Munk & MacDonald 1960). For a slowly convecting fluid such as a planetary mantle the inertial term $\partial \mathbf{H}/\partial t$ is negligible, so we may solve the simplified quasistatic equations

$$\mathbf{\Omega}(t) \times (\mathbf{I}(t) \cdot \mathbf{\Omega}(t)) = 0. \tag{2}$$

Equation (2) indicates that $\mathbf{\Omega}$ and $\mathbf{H}$ are parallel, so a solution for $\mathbf{\Omega}(t)$ is equivalent to solving an eigenvalue problem for $\mathbf{I}(t)$, where the eigenvectors correspond to the principal axes and the eigenvalues correspond to the principal moments (where the most stable orientation of the planet corresponds to rotating about the largest principal axis). In practice, this eigenvalue approach has been often used in previous studies for computing the spin axis of a planet (e.g. Steinberger & O'Connell 1997; Roberts & Zhong 2007). The moment of inertia tensor in Equation (2) includes all contributions to the mass structure of the planet, including the spherically symmetric mass distribution, rotational deformation, deformation due to self gravity, internal and surface density anomalies, and surface deflections due to density anomalies. Here we are interested in contributions from mantle convection, so we restrict our attention to these processes.

For mantle convection problems the moment of inertia tensor is commonly separated into three parts (Sabadini & Peltier 1981; Spada et al. 1992):

$$I_{ij}(t) = I_0 \delta_{ij} + J_{ij}(t) + E_{ij}(t) \tag{3}$$

where I_0 is the spherically symmetric reference moment, J_{ij} is the contribution due to rotational deformation, and E_{ij} is the contribution due to internal density anomalies, as well as the surface deflections caused by them. If we plug this decomposition into Equation (2) the spherically symmetric part $I_0 \delta_{ij}$ drops out, and we are left with

$$\mathbf{\Omega} \times (\mathbf{J} \cdot \mathbf{\Omega}) = -\mathbf{\Omega} \times (\mathbf{E} \cdot \mathbf{\Omega}). \tag{4}$$

This form of the quasistatic Liouville equation makes clear that the polar wander problem represents a balance between the mismatches of the convective part of the moment of inertia ($\mathbf{E}$) and the rotational deformation part of the moment of inertia ($\mathbf{J}$). Our goal is to characterize this balance from a perspective of scaling and fluid dynamics.

2.2 A note on reference frames

True polar wander can be described in different reference frames, and this choice is fundamentally an arbitrary one. However, certain aspects of the physics can be made much simpler by an appropriate choice of the reference frame. In our treatment of TPW, we will refer to three different reference frames:

First, there is the inertial, non-rotating frame corresponding to spatial coordinates that are fixed in time. Second, there is the body-fixed (or geographic) frame. By definition, the rotaiton of the body-fixed frame relative to the inertial frame is specified by $\mathbf{\Omega}$. A terrestrial no-net-rotation or hotspot reference frame are common choices for the body-fixed frame. Treatments of gravitational or rotational deformation of a planet are most naturally expressed in the body-fixed frame, as described in Section 2.3. Finally, there is the frame described by the principal axes of convective part of the moment of inertia $\mathbf{E}$, which we will refer to as the "$\mathbf{E}$-frame." Redistribution of mantle mass anomalies due to convection changes the principal axes of $\mathbf{E}$, rotating the $\mathbf{E}$-frame with respect to the geographic frame, which we will describe by a rotation vector $\mathbf{\Psi}$ (see Section 4.2).

These reference frames and vectors are illustrated in Figure 1.

2.3 Rotational deformation

The part of the moment of inertia due to the elastic rotational deformation in the body-fixed frame is traditionally related to the degree-two part of the gravity field via MacCullagh's formula (Munk & MacDonald 1960):

$$J_{ij} = \frac{ka^5}{3G}\left(\Omega_i\Omega_j - \frac{1}{3}\Omega_q\Omega_q\delta_{ij}\right) \tag{5}$$

where k is an elastic Love number, a is the semimajor axis of the planet, and G is the gravitational constant. This result may be extended to a viscoelastic rheology via the viscoelastic correspondence principle (e.g. Peltier 1974):

$$J_{ij} = \frac{k(t)a^5}{3G} * \left(\Omega_i\Omega_j - \frac{1}{3}\Omega_q\Omega_q\delta_{ij}\right) \tag{6}$$

where k is now a time-dependent viscoelastic Love number which is convolved with the time-dependent rotation vector.

The infinite-time limit of Equation (6) for a constant rotation vector around the z-axis implies

$$\begin{aligned} J_{zz} = C =& \frac{2}{3}\frac{k_f a^5 \Omega^2}{3G} \\ J_{xx} = J_{yy} = A =& -\frac{1}{3}\frac{k_f a^5\Omega^2}{3G} \end{aligned} \tag{7}$$

where C and A are the polar and equatorial moments of inertia, respectively, and k_f is the fluid limit of k. We can solve for k_f in terms of $C - A$:

$$k_f = \frac{3G(C-A)}{\Omega^2 a^5}. \tag{8}$$

This fluid-limit representation of the deformation does not allow for any disequilibrium between J_{ij} and E_{ij}, so it does not permit TPW.

Ricard et al. (1993) obtain an approximation to Equation (6) which retains its long-time behavior by entering the Laplace domain and truncating a Taylor series for $k(s)$ to first order. This introduces a new parameter, termed T_1, which can be seen as a weighted relaxation time for the system. This simple approximation in the Laplace domain allows for an analytical transformation back into the time domain, and neglecting second order terms in $\dot{\Omega}$ we find:

$$J_{ij} = \frac{k_f a^5}{3G}\left(\Omega_i\Omega_j - \frac{1}{3}\Omega_q\Omega_q\delta_{ij}\right) - \frac{k_f a^5 T_1}{3G}\left(\dot{\Omega}_i\Omega_j + \Omega_i\dot{\Omega}_j - \frac{2}{3}\Omega_q\dot{\Omega}_q\delta_{ij}\right). \tag{9}$$

The two terms of this equation have simple interpretations. The first term corresponds to the fluid limit of rotational deformation (in the absence of any long-term elastic strength). The second term represents the lag in the moment of inertia due to the viscous adjustment of the rotational bulge, where T_1 is the characteristic time constant for this adjustment. Since the first term represents the fluid limit of rotational deformation, it automatically satisfies Equation (2), and hence does not contribute to the polar wander problem.

2.4 The convective moment of inertia

The term on the right-hand side of Equation (4) represents the moment of inertia due to internal density anomalies as well as the surface deflections due to them. This, as well, may be parameterized using a viscoelastic Love number approach:

$$\mathbf{E} = \left[\delta(t) + k^L(t)\right] * \mathbf{C} \tag{10}$$

where k^L is an internal loading Love number representing the surface deflection due to density anomalies, and C_{ij} is the moment of inertia without that response. Frequently the simplification is made that the timescale of the surface response is quick compared to the true polar wander timescale, and we may use the fluid limit geoid kernels (e.g. Richards & Hager 1984):

$$E_{ij} = (1 + k_f^L)C_{ij}. \tag{11}$$

An alternative to the Love number formalism is to calculate to surface deflections directly using mantle convection simulations with a true free surface boundary condition. A recent implementation of a free surface boundary condition in the CIG-sponsored mantle convection software `ASPECT` (Rose et al. submitted) permits more general treatments of mantle rheology.

2.5 Rate of true polar wander

We are in a position to address the rates of true polar wander for a given convective moment $\mathbf{E}$. A considerable simplification occurs if we neglect secular changes in the rotation rate, and just consider changes in direction of the pole ($d\Omega^2/dt = 2\Omega_i\dot{\Omega}_i = 0$) Substituting Equation (9) into Equation (4) we find

$$\frac{k_f a^5 T_1 \Omega^2}{3G}\boldsymbol{\Omega}\times\dot{\boldsymbol{\Omega}} = \boldsymbol{\Omega}\times(\mathbf{E}\cdot\boldsymbol{\Omega}). \tag{12}$$

Introducing a unit vector $\boldsymbol{\omega} = \boldsymbol{\Omega}/\|\boldsymbol{\Omega}\|$ and using Equation (8) for k_f, we may solve this equation for $\dot{\boldsymbol{\omega}}$:

$$\dot{\boldsymbol{\omega}} = \frac{1}{(C-A)T_1}\left[\mathbf{E}\cdot\boldsymbol{\omega} - (\boldsymbol{\omega}\cdot\mathbf{E}\cdot\boldsymbol{\omega})\,\boldsymbol{\omega}\right]. \tag{13}$$

Note that the quantity in brackets is similar in form to the shear stress on a plane in classical elastostatics. This correspondence permits useful insights (see below). Let $\dot{\Theta} = |\dot{\boldsymbol{\omega}}|$ denote the rate of polar wander. Evaluating the scalar product $\dot{\Theta}^2 = \dot{\boldsymbol{\omega}}\cdot\dot{\boldsymbol{\omega}}$ gives

$$\dot{\Theta}^2 = \dot{\boldsymbol{\omega}}^2 = \frac{1}{(C-A)^2 T_1^2}\left[(\mathbf{E}\cdot\boldsymbol{\omega})^2 - (\boldsymbol{\omega}\cdot\mathbf{E}\cdot\boldsymbol{\omega})^2\right]. \tag{14}$$

The polar wander rate $\dot{\Theta}$ is measured in the body-fixed geographic frame, but the physics of the right-hand-side of Equation (14) is more naturally expressed in the reference frame of the principal axes of $\mathbf{E}$, which is, in general, rotating with respect to the geographic frame. However, the right-hand-side is scalar-valued, and as such is invariant to rotations. Therefore we can enter the coordinate system of the convective moment of inertia $\mathbf{E}$ with principal moments $\lambda_1 \leq \lambda_2 \leq \lambda_3$ and define the orientation of $\boldsymbol{\omega}$ with colatitude θ and longitude ϕ (see Figure 1). Plugging this description of $\boldsymbol{\omega}$ into Equation (14), and after some tedious algebra, we find

$$\begin{aligned}\dot{\Theta}^2 =& \frac{1}{4(C-A)^2T_1^2}\sin^2 2\theta\left[(\lambda_3-\lambda_1)^2\cos^2\phi + (\lambda_3-\lambda_2)^2\sin^2\phi\right] + \\ & \frac{1}{4(C-A)^2T_1^2}\sin^4\theta\sin^2 2\phi\,(\lambda_2-\lambda_1)^2.\end{aligned} \tag{15}$$

This equation is a version of what has been called the “Milankovitch theorem” (Munk & MacDonald 1960). Two special cases of this equation are of note. First, if $\dot{\Theta}^2$ is evaluated on the octahedral plane (the plane with direction cosines all $1/\sqrt{3}$, or $\phi = 45°, \theta \approx 55°$, cf. Fung (1965)), then it can be expressed in terms of the second invariant (E_{II}) of the moment of inertia deviator ($E_{ij} - 1/3E_{kk}\delta_{ij}$):

$$\begin{aligned}\dot{\Theta}^2 &= \frac{1}{9(C-A)^2T_1^2}\left[(\lambda_3-\lambda_1)^2 + (\lambda_3-\lambda_2)^2 + (\lambda_2-\lambda_1)^2\right] \\ &= \frac{E_{\mathrm{II}}}{9(C-A)^2T_1^2}.\end{aligned} \tag{16}$$

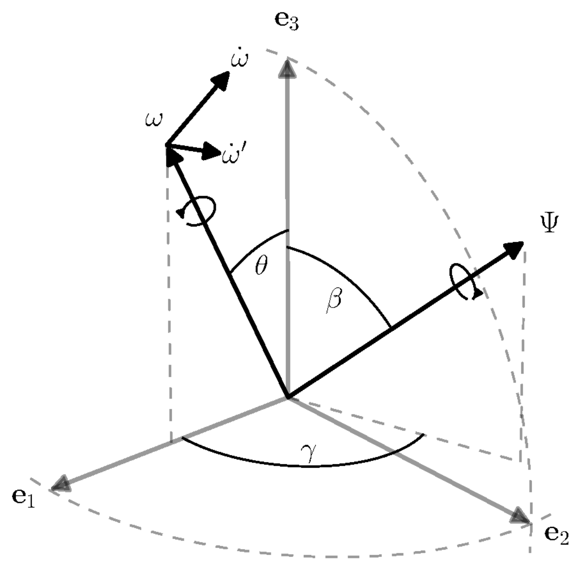

Figure 1. Relevant vectors and angles for the TPW analysis. The axes $\mathbf{e}_1$, $\mathbf{e}_2$, and $\mathbf{e}_3$ represent the principal axes of the convective moment of inertia $\mathbf{E}$, with associated eigenvalues λ_1, λ_2, and λ_3, respectively. Since the choice of geographic axes is arbitrary, we assume that at this instant the $\mathbf{E}$-frame and the geographic frames are colocated (though at future times they will not be). The angle θ represents the mismatch between the rotation axis $\boldsymbol{\omega}$ and the $\mathbf{e}_3$-axis. For illustration, we assume the longitude ψ of the rotation axis is zero so $\boldsymbol{\omega}$ lies in the $\mathbf{e_1}$-$\mathbf{e_3}$ plane. True polar wander in the geographic reference frame moves the rotation axis towards the $\mathbf{e}_3$-axis, shown by $\dot{\boldsymbol{\omega}}$. However, time-dependent convection in the mantle may cause a relative rotation between the geographic frame and the $\mathbf{E}$-frame. This relative rotation can be represented as a rotation around the axis $\boldsymbol{\Psi}$ in the geographic frame, which is defined by colatitude β and longitude γ. The rotation around the $\boldsymbol{\Psi}$ axis contributes to the motion of $\boldsymbol{\omega}$ as seen in the $\mathbf{E}$-frame. The motion of $\boldsymbol{\omega}$ in the $\mathbf{E}$-frame is shown by $\dot{\boldsymbol{\omega}}'$. Further discussion of the reference frames and the relative rotation vector $\boldsymbol{\Psi}$ can be found in Sections 2.2 and 4.2

The second invariant of the stress deviator is commonly used in the theories of elasticity and plasticity as a convenient scalar approximation of the shear stress in a system. The second invariant of the moment of inertia deviator can be similarly viewed as a scalar estimate of the "rotational stress."

The second special case is if the rotation vector $\boldsymbol{\omega}$ lies in $\mathbf{e}_1$-$\mathbf{e}_2$ plane ($\phi = 0$). Then Equation (15) becomes significantly simpler, which is useful for scaling purposes:

$$|\dot{\Theta}| = \frac{1}{2(C-A)T_1} \sin 2\theta(\lambda_3 - \lambda_1). \tag{17}$$

The maximum polar wander rate of the system is achieved when $\theta = 45°$ (see, e.g. Fung (1965)).

From Equation (17) it is clear that the important quantities for estimating $\dot{\Theta}$ are θ and the differences between the eigenvalues of the convective moment $\mathbf{E}$, both of which depend on the structure and dynamics of mantle convection. They represent, respectively, the size of convective anomalies in the moment of inertia tensor and the angular mismatch between the rotation axis and the principal axis of the convective moment. Both θ and λ_i depend upon the dynamics of the convecting planetary mantle. In order to derive estimates for them, we must consider those dynamics.

3 INTERNAL DYNAMICS

Mantle convection and rotational dynamics of planetary bodies are usually considered separately, yet the processes are based on a common set of governing equations. As such, some extra care must be taken to ensure that the equations we consider are self-consistent. Furthermore, since our goal is to establish a scaling for TPW rate, we must identify a minimal set of nondimensional numbers which describe its physics. For simplicty we consider an isoviscous planet in a rotating reference frame with no internal heating in the incompressible Boussinesq approximation. The equations for mass, momentum, and energy then read

$$\nabla \cdot \mathbf{u} = 0 \tag{18}$$

$$-\nabla P + \eta \nabla^2 \mathbf{u} = \rho \mathbf{g} - \rho \boldsymbol{\Omega} \times \boldsymbol{\Omega} \times \mathbf{r} \tag{19}$$

$$\frac{\partial T}{\partial t} + \mathbf{u} \cdot \nabla T = \kappa \nabla^2 T \tag{20}$$

where $\mathbf{u}$ is the velocity, P is the pressure, and T is the temperature. The gravity vector $\mathbf{g}$ is given by $\mathbf{g} = -\nabla V$, where the gravitational potential V comes from solving Poisson's equation

$$\nabla^2 V = 4\pi G \rho. \tag{21}$$

For the purposes of scaling, we assume that gravity is the approximately constant vector $g_0\hat{\mathbf{r}}$ (as is the case for Earth's mantle). In addition we use the simple equation of state

$$\rho = \rho_0 \left(1 - \alpha(T - T_0)\right). \tag{22}$$

The remaining parameters are defined in Table 1. Note that here we retain the centrifugal term, which is normally either neglected or absorbed into a modified pressure (in the latter case the boundary conditions on P must be modified). Dimensional analysis of this system (cf. Barenblatt (1996)) requires three nondimensional numbers to characterize it (a fourth one, defined by the ratio of the length of day to a diffusion timescale, does not appear in the governing equations). Convenient choices for these numbers are listed in Table 2, along with approximate Earth-like values for them.

In particular, the two most important numbers are the Rayleigh number, characterizing the vigor of convection, and the ratio of centrifugal to gravitational forces. This second nondimensional number does not have a uniformly agreed-upon name: it has been called a Froude number in analogy with other applications of inertial-to-gravitational effects (McKenzie 1968), and in the geodesy community has commonly been termed m (e.g. Nakiboglu 1982; Chambat et al. 2010), which we adopt here. Since we have begun with equations that do not have inertia or compressibility, we have implicitly thrown out the dependence on the nondimensional numbers that characterize those effects (e.g., the Prandtl and dissipation numbers). It would be straightforward to include them, but they do not affect the overall treatment of this scaling.

In this case the dynamics can be characterized in terms of deviations from a reference hydrostatic state, which includes the dynamic pressure $P^* = P - P_0$ and density perturbations $\delta\rho = \rho - \rho_0 = -\rho_0\alpha(T - T_0)$. In addition, we expect deviations in the figure of the planet from its hydrostatic shape, which we denote by $V = V_H + \Delta V$, where V_H is the hydrostatic figure and ΔV is the deviation. The introduction of ΔV requires another nondimensional number to characterize it, and we find that the quantity $\Gamma \equiv \alpha\Delta T$ is convenient. Finally, we define $\boldsymbol{\Omega} = \Omega_0\boldsymbol{\omega}$, where $\boldsymbol{\omega}$ is a unit vector in the direction of $\boldsymbol{\Omega}$.

By definition the hydrostatic reference state is a solution to Equation (19) where there is no flow:

$$-\nabla P_0 = \rho_0\mathbf{g} - \rho_0\boldsymbol{\Omega} \times \boldsymbol{\Omega} \times \mathbf{r}. \tag{23}$$

Nondimensionalizing with the parameters in Table 2 and removing the reference state we find the nondimensional momentum equation:

$$-\nabla P^* + \nabla^2\mathbf{u} - \mathrm{Ra}\, T\, \mathbf{g} + \mathrm{Ra}\, m\, T\, \boldsymbol{\omega} \times \boldsymbol{\omega} \times \mathbf{r} = 0. \tag{24}$$

We can explicitly draw the connection between the angular and linear momentum equations by returning to the dimensional Equation (19), crossing it with $\mathbf{r}$ and integrating over the volume of the mantle:

$$-\int_V \mathbf{r} \times \nabla P \, dV + \int_V \eta \mathbf{r} \times \nabla^2 \mathbf{u} \, dV - \int_V \rho \mathbf{r} \times \mathbf{g} \, dV + \int_V \rho \mathbf{r} \times \boldsymbol{\Omega} \times \boldsymbol{\Omega} \times \mathbf{r} \, dV = 0. \tag{25}$$

The first three terms represent pressure, viscous torques, and gravitational torques on the mantle. Convection in the outer core, atmospheres, and oceans is not strong enough to provide significant pressure and viscous torques over geologic timescales, and a self-gravitating body cannot self-torque (Braginsky & Roberts 1995). Therefore we can neglect those terms, and we are left with

$$\int_V \rho \mathbf{r} \times \boldsymbol{\Omega} \times \boldsymbol{\Omega} \times \mathbf{r} \, dV = 0 \tag{26}$$

which may be rewritten via the Jacobi identity to find

$$\boldsymbol{\Omega} \times \int_V \rho \mathbf{r} \times (\boldsymbol{\Omega} \times \mathbf{r}) \, dV = 0. \tag{27}$$

This can be directly identified with Equation (2), and is a statement that a quasistatic body will rotate around the principal axis of its total moment of inertia.

We now seek to evaluate Equation (26) in the perturbed, convecting state. Hydrostatic balance (Equation (23)) ensures that the integral over the reference shape V_H vanishes when $\rho = \rho_0$. Nonzero contributions arise from perturbations in the density field or from perturbations in the shape. To make this dependence explicit, we split the shape into the reference volume V_H and perturbations from it ΔV, and use Equation (22) to define density perturbations. Substituting this decomposition into Equation (26) brings the integral into the form

$$\begin{aligned} &\int_{V_H} \rho_0 \mathbf{r} \times \boldsymbol{\Omega} \times \boldsymbol{\Omega} \times \mathbf{r} \, dV + \int_{V_H} \rho_0 \alpha (T - T_0) \mathbf{r} \times \boldsymbol{\Omega} \times \boldsymbol{\Omega} \times \mathbf{r} \, dV + \\ &\int_{\Delta V} \rho_0 \mathbf{r} \times \boldsymbol{\Omega} \times \boldsymbol{\Omega} \times \mathbf{r} \, dV + \int_{\Delta V} \rho_0 \alpha (T - T_0) \mathbf{r} \times \boldsymbol{\Omega} \times \boldsymbol{\Omega} \times \mathbf{r} \, dV = 0. \end{aligned} \tag{28}$$

As previously noted, the first term of this equation is zero due to the hydrostatic equation. The fourth term is negligible due to being second order in the smallness parameters $\Delta V / V_H$ and $\Gamma \equiv \alpha \Delta T$. Removing these, we find

$$\int_{\Delta V} \rho_0 \mathbf{r} \times \boldsymbol{\Omega} \times \boldsymbol{\Omega} \times \mathbf{r} \, dV = -\int_{V_H} \rho_0 \alpha (T - T_0) \mathbf{r} \times \boldsymbol{\Omega} \times \boldsymbol{\Omega} \times \mathbf{r} \, dV. \tag{29}$$

This equation may be identified with Equation (4), where disequilibrium in the rotational deformation (left side) is balanced by the mismatch of the convective moment of intertia with the spin axis (right side). Our goal is to identify characteristic sizes of these quantities, which must be functions of the nondimensional numbers identified in Table 2.

Table 1. Parameters for rotating mantle convection

Symbol	Definition
R_i	inner radius
R	outer radius
G	gravitational constant
V	gravitational potential
M	mass of the planet
Ω_0	reference rotation rate
η	viscosity
κ	thermal diffusivity
α	thermal expansivity
g_0	reference gravity
I_0	reference moment of inertia
T_0	reference temperature
ρ_0	reference density
ΔT	temperature drop across mantle

4 SCALING

Having drawn the connection between the angular momentum equation (Section 2) and the linear momentum equation (Section 3), we would like to apply the scaling of the linear momentum equation to the problem of TPW. We would therefore like to rewrite Equation (17) in terms of the nondimensional numbers identified in Section 3. Specifically, we will need estimates for $(C - A)$, T_1, $(\lambda_3 - \lambda_1)$, and θ.

It is useful to define a nondimensional eigenvalue difference (or "eigengap") $\Lambda_{ij} \equiv (\lambda_i - \lambda_j)/I_0$. This quantity represents the size of fluctuations in the convective moment of inertia compared to the reference value. The difference in the polar and equatorial moments of the hydrostatic planet $(C - A)$ is proportional to the ratio of rotational to gravitational forces((Munk & MacDonald 1960):

$$(C - A) \sim I_0 m. \tag{30}$$

Table 2. Nondimensional numbers with approximate Earth-like values

Symbol	Name	Definition	Approximate value
Ra	Rayleigh	$\rho_0 g_0 \alpha \Delta T R^3/\eta\kappa$	10^7
m	Froude	$\Omega_0^2 R/g_0 = \Omega_0^2 R^3/GM$	10^{-3}
A	aspect ratio	R_i/R	0.54
Γ	density deficit	$\alpha\Delta T$	10^{-2}

The time constant T_1 is a viscous relaxation time of the planetary mantle. It is frequently represented as a weighted average of the different relaxation modes (e.g. Ricard et al. 1993; Greff-Lefftz 2004), but for our purposes it is enough to approximate it as a single mode:

$$T_1 \sim \frac{\eta}{\rho_0 g_0 R} = \frac{R^2}{\kappa} \frac{\Gamma}{\mathrm{Ra}}. \tag{31}$$

Plugging these scalings into Equation (17) we find

$$\frac{\kappa}{R^2} \dot{\Theta} \sim -\frac{\mathrm{Ra}}{\Gamma m} \Lambda_{31} \sin 2\theta. \tag{32}$$

At this point we do not have estimates for the characteristic magnitudes of Λ_{ij} or θ, both of which are crucial for predicting characteristic rates of TPW. They represent, respectively, the size of convective anomalies in the moment of inertia tensor and the angular mismatch between the rotation axis and the principal axis of the convective moment.

The quantites Λ_{ij} and θ should be functions of our nondimensional parameters Ra, m, and Γ. We consider relatively slowly rotating bodies here ($m \ll 1$), and so make the simplifying assumption that the rotation does not significantly affect the style of convection. In this regime, therefore, we neglect the dependence on m, and look for scalings of the form $\Lambda_{ij}(\mathrm{Ra}, \Gamma)$ and $\theta(\mathrm{Ra}, \Gamma)$.

4.1 An estimate of Λ_{ij}

Fluctuations in the nonhydrostatic moment of inertia are due to temperature fluctuations in the mantle and their spatial structure:

$$C_{ij} = \int_{V_S} \rho_0 \alpha (T - T_0) \left(r_q r_q \delta_{ij} - r_i r_j \right) \, dV \tag{33}$$

where V_S is the reference spherical volume of the mantle. As discussed in Section 2.4, these internal density loads may be convolved with their surface responses to get the convective moment of inertia E_{ij}. The surface response is a function of the viscosity structure of the planet and the wavelength and depth of the interal load. The factor $(1 + k_f^L)$ is generally an order-one parameter (strictly speaking, dynamic compensation usually makes it less than one, (e.g. Richards & Hager 1984)). For the purposes of scaling it is reasonable to neglect this multiplicative factor.

For thermal convection, the convective part of the moment of inertia E_{ij} is directly related to the degree-two part of the temperature field (see Appendix A). Therefore, an estimate of one allows an estimate of the other. We can expand the temperature structure of the convecting planet with a set of orthonormal basis functions $R_n Y_{lm}$, where Y_{lm} are spherical harmonics, R_n are some set of orthogonal

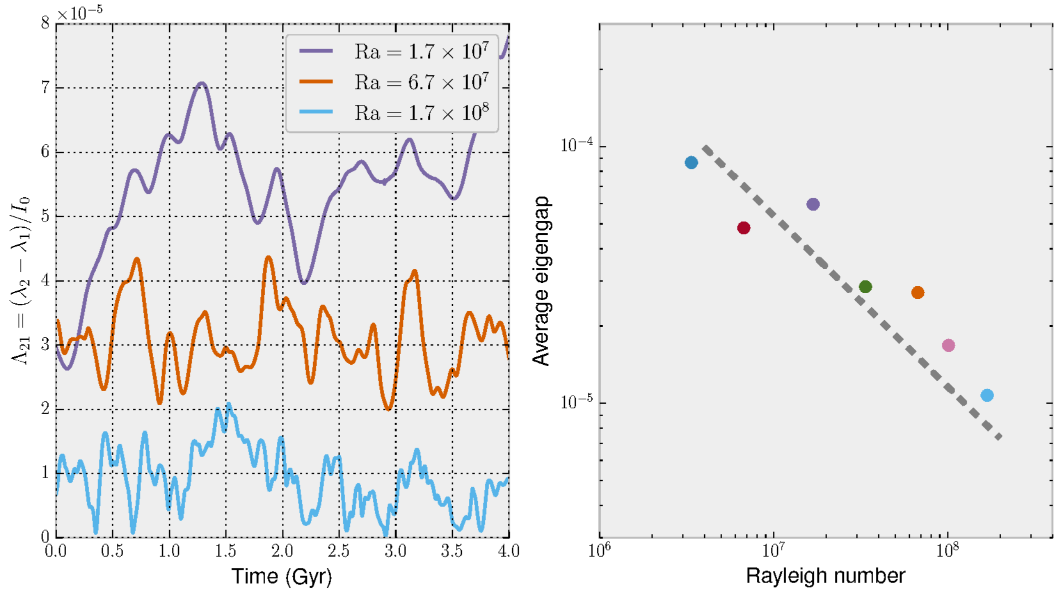

Figure 2. Left: Time series of the normalized difference between moments $\Lambda_{21} = (\lambda_2 - \lambda_1)/I_0$ for convection in a 2D annulus at several different Rayleigh numbers. As the Rayleigh number increases, the average value of the relative moment decreases due to less low-degree coherence in the temperature structure. Right: average value of Λ_{21} for the different Rayleigh numbers. Also shown is a line with slope $\mathrm{Ra}^{-2/3}$, which is predicted from the scaling analysis (the exponent is $-2/3$ instead of -1 due to the reduced dimensionality of the simulations).

radial polynomials, and T_{nlm} are the coefficents for the expansion which have been normalized by ΔT:

$$T(r, \theta, \phi, t) = \Delta T \sum_{n=0}^{\infty} \sum_{l=0}^{\infty} \sum_{m=-l}^{l} T_{lmn}(t) R_n(r) Y_{lm}(\theta, \phi). \tag{34}$$

Inserting the temperature expansion (34) into Equation (33) results in a prefactor of the nondimensional number $\Gamma = \alpha \Delta T$. Orthogonality of the basis functions for the expansion means that the integral for C_{ij} picks out degree-two spherical harmonics in the lateral dimensions, and only the lowest few radial functions $R_n(r)$. Therefore, of the entire temperature spectrum, only a few of the modes matter for TPW. We want to estimate the power in those few modes, which we denote by $T_{\text{degree-two}}$ (see Appendix A for more detail):

$$\Lambda_{31} \sim \Gamma T_{\text{degree-two}}. \tag{35}$$

The temperature field has been normalized by ΔT and thus goes between zero and one, therefore the expansion in T_{lmn} is constrained by

$$\max \left(\sum_{n=0}^{\infty} \sum_{l=0}^{\infty} \sum_{m=-l}^{l} T_{lmn}(t) R_n(r) Y_{lm}(\theta, \phi) \right) = 1. \tag{36}$$

This is a strong constraint, but it gives very little information about the distribution of power across the

T_{lmn}. We can, however, think about the power spectrum in two different regimes: that of steady/quasisteady flow (relatively low Ra) and that of chaotic flow (relatively high Ra). The structure of thermal convection is primarily controlled by the Rayleigh number. Once the Rayleigh number is sufficiently high ($\sim 10^6$) the style of convection changes from steady/quasisteady to chaotic. Accompanying this transition to chaos is a broadening of the spatial and temporal spectra (McLaughlin & Orszag 1982).

At low Rayleigh number we expect the spectrum of the temperature field to be dominated by only a few low-degree modes which are largely influenced by the aspect ratio. This spectrum may or may not have a lot of power in the degree-two modes, and does not depend strongly on time.

At high Rayleigh number we expect the shortest lengthscales to be limited by the effects of thermal diffusion, which tends to wipe out thermal heterogeneity at small scales. Consequently, there will be little power in modes with shorter lengthscales than that allowed by diffusion. Therefore we expect, to a good approximation, that the infinite sum in Equation (34) can be truncated at some maximum wavenumber, set by the smallest lengthscale d:

$$n_{\max}, l_{\max}, m_{\max} \sim \frac{R}{d}. \tag{37}$$

Strictly speaking, convective mixing can produce smaller scales, but the power in these scales is greatly reduced by diffusion. Thus total number of modes that are accessible to the system are

$$N_{\text{modes}} = n_{\max} \times l_{\max} \times m_{\max} \sim \left(\frac{R}{d}\right)^3. \tag{38}$$

The value of each $T_{lmn}(t)$ will in general be some complex function of time, but for a given style of convection we expect there to be some average value. For chaotic flow the power should be spread out amongst the modes accessible to it. We may make the hypothesis that each of the modes are roughly as likely as any of the others, which implies

$$T_{\text{degree-two}}(t) \sim \frac{1}{N_{\text{modes}}} \sim \left(\frac{d}{R}\right)^3. \tag{39}$$

Any of a number of scaling laws can provide an estimate for the characteristic length scale of a convecting system which may depending on rheology, geometry, or density structure. The simplest, based on boundary layer theory (Turcotte & Oxburgh 1967), finds $d/R \sim \mathrm{Ra}^{-1/3}$. This scaling is roughly a measure of the diffusive lengthscale for the timescale of a convective overturn, consistent with the cutoff in Equation (37). It thus furnishes us with an estimate of the power in the degree-two part of the field as a function of Rayleigh number:

$$T_{\text{degree-two}}(t) \sim \mathrm{Ra}^{-1}. \tag{40}$$

We performed a series of numerical simulations of mantle convection at different Rayleigh numbers to test this scaling. We used the mantle convection software `ASPECT` (Kronbichler et al. 2012), based on the finite element library `deal.II` (Bangerth et al. 2015). which allows for flexible implementation of different rheologies, geometries, and postprocessors. In order to test a wide range of Rayleigh numbers, we ran the simulations in a 2D annulus, tracking the eigenvalues of the moment of inertia tensor and integrating Equation (13) in time. For the 2D simulations there is a reduced dimensionality when calculating the number of modes, so $N_{\text{modes}} \sim (R/d)^2$. This leads us to a scaling of $T_{\text{degree-two}} \sim \text{Ra}^{-2/3}$, which is shown as a dashed line in Figure 2. This result has a simple interpretation. As the Rayleigh number of the system increases, the smallest lengthscale of convective features gets smaller. The total power in the temperature field is spread across a larger spectrum, leaving less total power for the degree-two part, which is what drives TPW.

With an estimate for the power in the degree-two part of the temperature field, we may finally estimate Λ_{ij}:

$$\Lambda_{ij} \sim \frac{\Gamma}{\text{Ra}}. \tag{41}$$

Other power spectra for the temperature field are possible. Isoviscous models tend to be "bluer," and models with viscosity stratification tend to be "redder" (Richards et al. 1999). Present day Earth seems to have a fairly "red" spectrum, with large low-degree seismic anomalies due to Cenozoic subduction history and the lower mantle LLSVPs (Dziewonski et al. 2010). Nevertheless, at high Rayleigh number the expectation is that the power will be distributed across many length scales.

4.2 Estimating the mismatch θ

The mismatch between the current rotation axis and the principal axis of the convective moment is perhaps the most important parameter in Equation (32). Much of the debate around the existence and magnitude of TPW on Earth comes down to the question of how big θ can be (Kirschvink et al. 1997; Steinberger & O'Connell 1997).

There are two processes at work which control the evolution of θ, its growth through perturbations in the convective moment and its decay via relaxation of the pole towards the maximum moment of inertia. We can explore these two effects by converting Equation (13) from the body-fixed frame to the $\mathbf{E}$-frame (recall that $\mathbf{\Omega}$ defines the rotation of the body-fixed frame relative to inertial space, as shown in Equation (1)). The $\mathbf{E}$-frame slowly rotates with respect to the geographic frame, described by the rotation vector $\mathbf{\Psi}$ (here $\mathbf{\Psi}$ defines the rotation of the $\mathbf{E}$-frame in the geographic frame, see Figure 1). We can then write the rate of change of $\boldsymbol{\omega}$ in the $\mathbf{E}$-frame (denoted by primes)

$$\dot{\boldsymbol{\omega}} = \dot{\boldsymbol{\omega}}' + \mathbf{\Psi} \times \boldsymbol{\omega}'. \tag{42}$$

Equation (13) then becomes

$$\dot{\boldsymbol{\omega}}' = \frac{1}{(C-A)T_1}\left[\mathbf{E}'\cdot\boldsymbol{\omega}' - \left(\boldsymbol{\omega}'\cdot\mathbf{E}'\cdot\boldsymbol{\omega}'\right)\boldsymbol{\omega}'\right] - \boldsymbol{\Psi}\times\boldsymbol{\omega}'. \tag{43}$$

The advantage of expressing TPW in the $\mathbf{E}$-frame is that the entire equation may be written in terms of the principal moments λ_i and the angles from the principal axes. As in Equation (17), we make the simplifying assumption that $\phi = 0$ (for nonzero ϕ the equations become more complex, but the basic physics is unchanged). The direction of Ψ is given by colatitude β and longitude γ, as shown in Figure 1.

We may solve Equation (43) for $\dot{\theta}$ (i.e., the colatitudinal velocity in the $\mathbf{E}$ frame, not the TPW rate $\dot{\Theta}$) in terms of θ, β, and γ:

$$\dot{\theta} = -\frac{1}{2(C-A)T_1}\sin 2\theta(\lambda_3 - \lambda_1) - |\boldsymbol{\Psi}|\sin\beta\sin\gamma. \tag{44}$$

Equation (44) captures the essential competition between growth and decay of the mismatch angle. The first term acts to reduce θ via TPW, while the second term can increase (or decrease) it arbitrarily via relative motion between the geographic frame and the principal axes of the $\mathbf{E}$-frame. Comparison with Equation (17) shows that, when $|\boldsymbol{\Psi}|$ is zero, then the rate of TPW $|\dot{\Theta}|$ is identical to $|\dot{\theta}|$. Conversely, when the rate of TPW is very slow (i.e. $|\dot{\Theta}| \sim 0$), then $|\dot{\theta}| \sim |\boldsymbol{\Psi}|$ and θ is completely determined by $\boldsymbol{\Psi}$ (where we have neglected the orientation factor $\sin\beta\sin\gamma$ for the purposes of scaling). In order for the TPW rate to be large, the growth of θ via $|\boldsymbol{\Psi}|$ must, at least occasionally, be larger than its decay.

An estimate for $|\boldsymbol{\Psi}|$ must concern the stability of the convective moment of inertia. Convection is continuously redistributing mass throughout the mantle, which will perturb the convective moment of inertia. If the convective moment is stable to small perturbations, then $|\boldsymbol{\Psi}|$ should be small, and θ will never be large. However, if $\mathbf{E}$ is not stable to perturbations, then θ could be up to $90°$. Given a random perturbation to $\mathbf{E}$, we would like to give a bound on the size of the perturbation to θ. This may be done by application of a theorem due to Davis & Kahan (1970).

Let δ be the size of the perturbation to the convective moment of inertia tensor, and let $\lambda_3 \geq \lambda_2 \geq \lambda_1$ be the eigenvalues of that tensor. Then the rotation of the principal axes of the tensor is bounded by

$$|\sin(2\theta)| \leq \frac{2|\delta|}{\min\limits_{i\neq j}|\lambda_i - \lambda_j|}. \tag{45}$$

That is to say, if there is a large difference between the eigenvalues, this stabilizes axes to perturbations. If, however, there is a small difference between the eigenvalues (i.e., they are nearly degenerate), then perturbations can cause large rotations of the principal axes. This is illustrated schematically in Figure 3

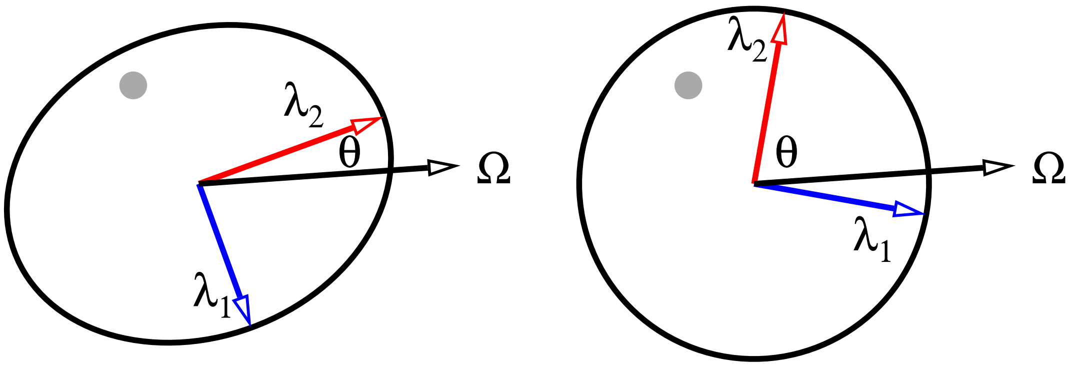

Figure 3. Graphical demonstration of the $\sin 2\theta$ theorem of Davis & Kahan (1970). Two spheroidal bodies with eigenvalues $\lambda_2 > \lambda_1$ start out with the rotation axis Ω aligned with the λ_2 axis. However, on the left the eigengap $\|\lambda_2 - \lambda_1\|$ is large, while on the right it is small. A negative mass perturbation is instantaneously added to both bodies, which effects a small rotation of the principal axes on the left, but a large one on the right.

249 We may arrive at a simple estimate of the growth rate of the angle θ (and thus $|\mathbf{\Psi}|$) by differenti-
250 ating Equation (45), tentatively holding $|\lambda_i - \lambda_j|$ fixed:

$$|\mathbf{\Psi}| \sim |\dot{\theta}| \leq \frac{|\dot{\delta}|}{\min\limits_{i \neq j} |\lambda_i - \lambda_j|}. \tag{46}$$

251 The quantity $(\lambda_i - \lambda_j)$ which appears in the denominator of these equations is precisely the same
252 as the quantity which we estimated in the previous section to scale with $\sim \mathrm{Ra}^{-1}$. Therefore, as the
253 Rayleigh number increases, the characteristic gap between the eigenvalues of the convective moment
254 becomes smaller. Additionally, the timescale of fluctuations in these values goes down. Overall, this
255 makes the principal axes of high Rayleigh number systems much less stable. This is consistent with
256 the result of Richards et al. (1999).

257 In the limit that the eigengap becomes zero, the rotation of the pinciple axes can be arbitrary. This
258 essentially corresponds to the hypothesized “inertial interchange true polar wander” (Kirschvink et al.
259 1997), where the mismatch angle is $90°$. However, the eigengap does not need to be zero for there to
260 be large displacements polar wander, and if it does go to zero, the wander does not need to be $90°$.

261 Figure 4 shows a representative timeseries for annular convection, where we track the eigenvalues
262 of the moment of inertia and integrate Equation (13) in time. Since it is a 2D model, the spin axis
263 may be represented by a single angle. When the eigengap gets small, the misfit angle becomes much
264 larger, and the rate of polar wander becomes much faster. At $\sim$1 Gyr the eigengap goes to zero, and
265 the misfit angle goes to approximately $90°$, an IITPW event. But there are several other events where
266 the eigengap becomes small, and there are still large TPW events associated with them. For example,

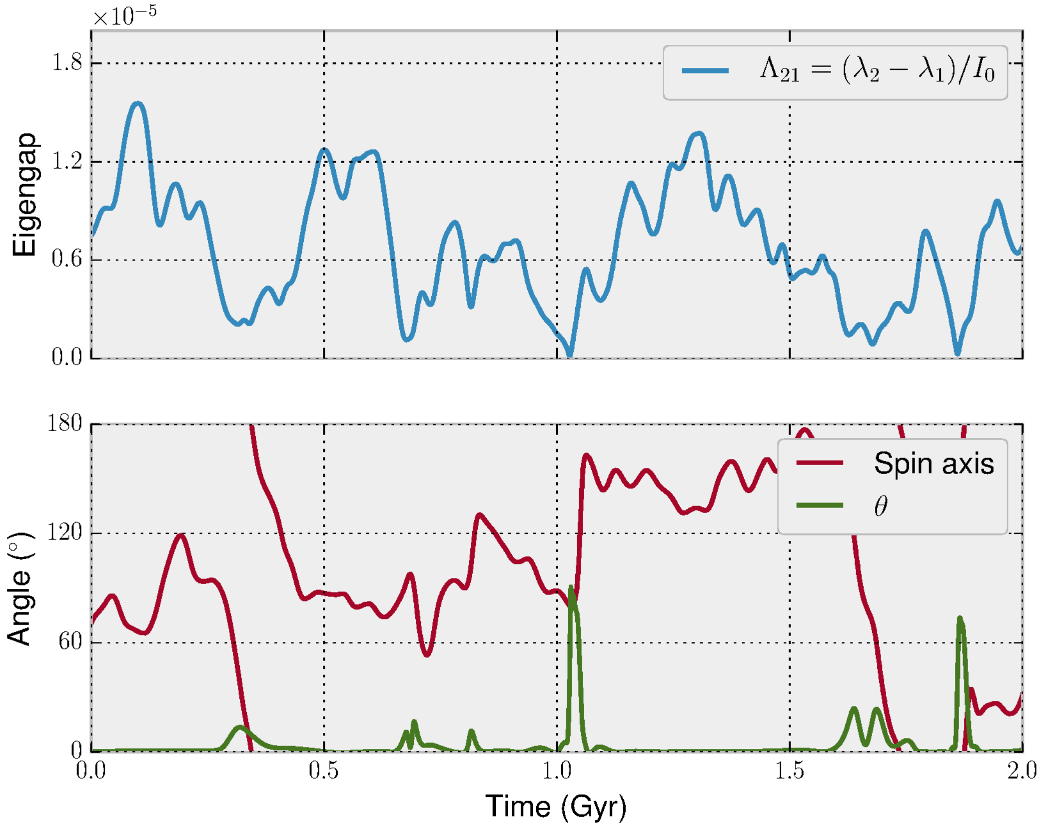

Figure 4. Top: Time series of principal moments for 2D annular convection at $\mathrm{Ra} \sim 10^8$. Bottom: Time series of spin axis and mismatch angle θ. When the two moments are close to each other (small eigengap), the mismatch angle becomes large, and the rate of polar wander is significantly larger. At $\sim$1 Gyr the gap goes to zero and there is a nearly $90°$ TPW event, with $\sim 80°$ degrees of polar wander in $\sim$30 Myr. However, there are several other large TPW events which happen when the eigengap is small.

at $\sim$0.3 Gyr the eigengap dips, with an associated large TPW event, even though there is technically no interchange of the axes.

We suggest, then, that $90°$ IITPW events are simply a special case of a broad class of events which can occur when the principal moments are close to each other. Furthermore, a more vigorously convecting planet is much more likely to experience rapid TPW events as it has a lower characteristic gap between principal moments and the gap is much more likely to go to zero.

5 DISCUSSION

The preceding results clarify the complex relationship between the Rayleigh number, m, and the rates of TPW for a convecting planet. As mantle convection redistributes mass in the planet's interior, the rotational bulge moves around to stay aligned with the principal axes of the convective moment of inertia. There is a constant competition between growth of the mismatch angle θ through Equation (46) and its relaxation through Equation (17). We may plug in the estimate for Λ_{ij} (Equation (41)) into Equation (17) to find the strikingly simple expression

$$\frac{\kappa}{R^2}\,\dot{\Theta} \sim -\frac{1}{m}\sin 2\theta. \tag{47}$$

Surprisingly, Γ and Ra have completely dropped from the prefactor in the scaling. Response timescales for relaxation of the mismatch angle go down at high Rayleigh numbers. At the same time, however, coherence in the temperature structure goes down, reducing the amount of power in the degree-two part of the field responsible for driving TPW. That these two effects cancel is something of a coincidence due to the simple estimate of the smallest lengthscales of the problem. Scalings for lengthscales of convection in fluids with temperature dependent viscosity (e.g. Solomatov 1995) or pseudoplastic rheology (e.g. Korenaga 2010) have different functional dependencies on Ra or additional nondimensional parameters. However, a common feature in most scalings is that typical lengthscales are still some power-law of Rayleigh number $d \propto \mathrm{Ra}^{-\beta}$. With this form, our scaling for TPW rate has the following dependence on Ra:

$$\frac{\kappa}{R^2}\,\dot{\Theta} \sim -\frac{\mathrm{Ra}^{1-3\beta}}{m}\sin 2\theta. \tag{48}$$

In general, β is some small number between one-fourth and one-third, so we expect that more complicated estimates for $d(\mathrm{Ra})$ will still result in a weak dependence of the prefactor in Equation (48) on the Rayleigh number.

We then suggest that the most important parameters are m, which acts as the brakes on the system, and the mismatch angle $\theta(\mathrm{Ra})$. Whereas the rest of the expression has a weak dependence on Ra, θ is expected to be strongly dependent on it.

Indeed, we can identify two endmember behaviors of Equation (48). When convection is not sufficiently chaotic to create a large θ we are in the regime where the planet's rotation axis closely tracks that of the convective moment. This is the regime considered in Steinberger & O'Connell (1997), Roberts & Zhong (2007), and Zhong et al. (2007), and can be considered the "slow TPW" regime. When convection is more chaotic, however, there may be large excursions in θ, which can drastically increase the wander rate. If $\theta = 90°$, this corresponds to IITPW (Kirschvink et al. 1997). This, however, is a special case in the large θ, "fast TPW" regime.

As an example, we may consider the early Earth, when the mantle was presumably hotter and less viscous, leading to a higher Rayleigh number. We would then predict that convection was more vigorous, leading to a less stable $\theta(t)$, and thus more TPW and more frequent "fast TPW" events.

For Cenozoic Earth we can substitute direct estimates of the important parameters into Equation (17). Typical values for the time constant T_1 are of order $30\,\mathrm{kyr}$ (Ricard et al. 1993). Estimates of the present day non-hydrostatic moment of inertia (due to mantle density anomalies, corresponding to $\Lambda_{31} I_0$ in the preceding scaling) are in the neighborhood of $10^{-5} I_0$, while the hydrostatic moment of inertia (corresponding to $C - A$) is $3 \times 10^{-3} I_0$ (Chambat & Valette 2001). A key question is whether convection is sufficiently chaotic to enter the large θ regime. Richards et al. (1997) have argued that the convective planform of Earth has been stable for the last few hundred million years. On the other hand, we know that there have been large reorganizations of that planform during Earth history, so this recent geologic stability may not hold in general (Evans 2003). Our numerical simulations show that large values for θ are possible in a vigorously convecting mantle. Allowing for such a large mismatch angle ($\theta = 45°$) we may estimate the maximum polar wander rate

$$\max(\dot{\Theta}) = \frac{(\lambda_3 - \lambda_1)}{(C - A)} \frac{1}{T_1} \sim 6°/\mathrm{Myr} \tag{49}$$

which is similar to the timescales discussed by Cambiotti et al. (2011), and within the range suggested by paleomagnetic observations. The bulk viscosity of Earth's mantle is uncertain by up to a factor of ten (Mitrovica & Forte 2004), which results in a corresponding uncertainty for the relaxation time T_1 and the maximum polar wander rate.

Thus far we have restricted our discussion to planets with lithospheres lacking long-term elastic strength. For this case the long-time limit of the planetary figure is coaxial with the convective moment of inertia. This assumption is not necessarily true in all cases. Earth's lithosphere is pervasively fractured and hydrated, and may not have much strength when subjected to rotational changes on geologic timescales. However, a planet with a stagnant lid (such as Mars) may have considerable strength, preventing the figure of the planet from reaching the fluid limit of Equation (8).

The theory of TPW response for the case of elastic lithospheres has been developed in, among other places, Matsuyama et al. (2006), Creveling et al. (2012), and Chan et al. (2014). The formalism developed in Section 4 can still be applied to this case, though the response to internal variations in the moment of inertia becomes more limited (and potentially richer, as in the oscillitory motions suggested by Creveling et al. (2012)).

6 CONCLUSION

We have developed a framework for discussing the rates of true polar wander for a convecting planet from a perspective of scaling and fluid dynamics. We identified a small number of dimensionless parameters which describe the system, and showed how they affect the overall dynamics of the system.

The most important parameters are the Rayleigh number and m, which acts as a damper to TPW. The dependence on the Rayleigh number is more complicated, since it is a control on both the forcing of TPW and the response, which act in opposite directions. Overall, however, we expect that more vigorously convecting planets should be less rotationally stable, and experience more TPW. This perspective allows us to consider not only the polar wandering of Phanerozoic Earth, but also allows us to hypothesize about polar wandering during the Archean and Proterozoic, or on other planetary bodies.

ACKNOWLEDGMENTS

This work was supported by National Science Foundation grant EAR-1246670. We thank Yanick Ricard for a thoughtful review.

REFERENCES

Bangerth, W., Heister, T., Heltai, L., Kanschat, G., Kronbichler, M., Maier, M., Turcksin, B., & Young, T. D., 2015. The `deal.II` library, version 8.2, *Archive of Numerical Software*, **3**.

Barenblatt, G. I., 1996. *Scaling, self-similarity, and intermediate asymptotics: dimensional analysis and intermediate asymptotics*, Cambridge University Press.

Braginsky, S. I. & Roberts, P. H., 1995. Equations governing convection in earth's core and the geodynamo, *Geophysical & Astrophysical Fluid Dynamics*, **79**(1-4), 1–97.

Cambiotti, G., Ricard, Y., & Sabadini, R., 2011. New insights into mantle convection true polar wander and rotational bulge readjustment, *Earth and Planetary Science Letters*, **310**(3), 538–543.

Chambat, F. & Valette, B., 2001. Mean radius, mass, and inertia for reference earth models, *Physics of the Earth and Planetary Interiors*, **124**(3), 237–253.

Chambat, F., Ricard, Y., & Valette, B., 2010. Flattening of the earth: further from hydrostaticity than previously estimated, *Geophysical Journal International*, **183**(2), 727–732.

Chan, N.-H., Mitrovica, J., Daradich, A., Creveling, J., Matsuyama, I., & Stanley, S., 2014. Time-dependent rotational stability of dynamic planets with elastic lithospheres, *Journal of Geophysical Research: Planets*, **119**(1), 169–188.

Creveling, J., Mitrovica, J., Chan, N.-H., Latychev, K., & Matsuyama, I., 2012. Mechanisms for oscillatory true polar wander, *Nature*, **491**(7423), 244–248.

Dahlen, F., Tromp, J., & Lay, T., 1999. Theoretical global seismology, *Physics Today*, **52**, 61.

Darwin, G., 1887. On the influence of geological changes on the earth's axis of rotation, *Philosophical Transactions of the Royal Society*.

Davis, C. & Kahan, W. M., 1970. The rotation of eigenvectors by a perturbation. iii, *SIAM Journal on Numerical Analysis*, **7**(1), 1–46.

Dziewonski, A. M., Lekic, V., & Romanowicz, B. A., 2010. Mantle anchor structure: An argument for bottom up tectonics, *Earth and Planetary Science Letters*, **299**(1), 69–79.

Evans, D. A., 2003. True polar wander and supercontinents, *Tectonophysics*, **362**(1), 303–320.

Fung, Y.-c., 1965. *Foundations of solid mechanics*, Prentice Hall.

Goldreich, P. & Toomre, A., 1969. Some remarks on polar wandering, *Journal of Geophysical Research*, **74**(10), 2555–2567.

Greff-Lefftz, M., 2004. Upwelling plumes, superswells and true polar wander, *Geophysical Journal International*, **159**(3), 1125–1137.

Kirschvink, J. L., Ripperdan, R. L., & Evans, D. A., 1997. Evidence for a large-scale reorganization of early cambrian continental masses by inertial interchange true polar wander, *Science*, **277**(5325), 541–545.

Korenaga, J., 2010. Scaling of plate tectonic convection with pseudoplastic rheology, *Journal of Geophysical Research: Solid Earth (1978–2012)*, **115**(B11).

Kronbichler, M., Heister, T., & Bangerth, W., 2012. High accuracy mantle convection simulation through modern numerical methods, *Geophysical Journal International*, **191**(1), 12–29.

Matsuyama, I., Mitrovica, J. X., Manga, M., Perron, J. T., & Richards, M. A., 2006. Rotational stability of dynamic planets with elastic lithospheres, *Journal of Geophysical Research: Planets*, **111**(E2), n/a–n/a, E02003.

McKenzie, D., 1968. The influence of the boundary conditions and rotation on convection in the earth's mantle, *Geophysical Journal International*, **15**(5), 457–500.

McLaughlin, J. B. & Orszag, S. A., 1982. Transition from periodic to chaotic thermal convection, *Journal of Fluid Mechanics*, **122**, 123–142.

Mitchell, R. N., Kilian, T. M., Raub, T. D., Evans, D. A., Bleeker, W., & Maloof, A. C., 2011. Sutton hotspot: Resolving ediacaran-cambrian tectonics and true polar wander for laurentia, *American Journal of Science*, **311**(8), 651–663.

Mitrovica, J. & Forte, A., 2004. A new inference of mantle viscosity based upon joint inversion of convection and glacial isostatic adjustment data, *Earth and Planetary Science Letters*, **225**(1), 177–189.

Munk, W. & MacDonald, G., 1960. *The Rotation of the Earth, 323*, Cambridge University Press, New York.

Nakiboglu, S., 1982. Hydrostatic theory of the earth and its mechanical implications, *Physics of the Earth and Planetary Interiors*, **28**(4), 302–311.

Peltier, W., 1974. The impulse response of a maxwell earth, *Reviews of Geophysics*, **12**(4), 649–669.

Ricard, Y., Spada, G., & Sabadini, R., 1993. Polar wandering of a dynamic earth, *Geophysical Journal International*, **113**(2), 284–298.

Richards, M., Bunge, H.-P., Ricard, Y., & Baumgardner, J., 1999. Polar wandering in mantle convection models, *Geophysical research letters*, **26**(12), 1777–1780.

Richards, M. A. & Hager, B. H., 1984. Geoid anomalies in a dynamic earth, *Journal of Geophysical Research: Solid Earth (1978–2012)*, **89**(B7), 5987–6002.

Richards, M. A., Ricard, Y., Lithgow-Bertelloni, C., Spada, G., & Sabadini, R., 1997. An explanation for earth's long-term rotational stability, *Science*, **275**(5298), 372–375.

Roberts, J. H. & Zhong, S., 2007. The cause for the north–south orientation of the crustal dichotomy and the equatorial location of tharsis on mars, *Icarus*, **190**(1), 24–31.

Rose, I., Buffett, B., & Heister, T., submitted. Free surface calculations in mantle convection.

Sabadini, R. & Peltier, W., 1981. Pleistocene deglaciation and the earth's rotation: implications for mantle viscosity, *Geophysical Journal International*, **66**(3), 553–578.

Solomatov, V., 1995. Scaling of temperature-and stress-dependent viscosity convection, *Physics of Fluids (1994-present)*, **7**(2), 266–274.

Spada, G., Ricard, Y., & Sabadini, R., 1992. Excitation of true polar wander by subduction, *Nature*, **360**(6403), 452–454.

Steinberger, B. & O'Connell, R. J., 1997. Changes of the earth's rotation axis owing to advection of mantle density heterogeneities, *Nature*, **387**(6629), 169–173.

Tsai, V. C. & Stevenson, D. J., 2007. Theoretical constraints on true polar wander, *Journal of geophysical research*, **112**(B5), B05415.

Turcotte, D. & Oxburgh, E., 1967. Finite amplitude convective cells and continental drift, *Journal of Fluid Mechanics*, **28**(01), 29–42.

Zhong, S., Zhang, N., Li, Z.-X., & Roberts, J. H., 2007. Supercontinent cycles, true polar wander, and very long-wavelength mantle convection, *Earth and Planetary Science Letters*, **261**(3), 551–564.

APPENDIX A: DEGREE-TWO MOMENTS

There is a connection between the moment of inertia of a rotating object and the degree-two density structure. The moment of inertia tensor may be written in index notation

$$I_{ij} = \int_V \rho \left(r_q r_q \delta_{ij} - r_i r_j \right) dV \tag{A.1}$$

where $\mathbf{r}$ is the Eulerian coordinate, ρ is the density, and V is the volume of the material. It is useful to enter the principal axes of the moment of inertia:

$$\mathbf{I} = \mathbf{1} \begin{bmatrix} \lambda_1 \\ \lambda_2 \\ \lambda_3 \end{bmatrix} = \mathbf{1} \begin{bmatrix} \int_V \rho(y^2 + z^z) dV \\ \int_V \rho(x^2 + z^2) dV \\ \int_V \rho(x^2 + y^2) dV \end{bmatrix} \tag{A.2}$$

where $\mathbf{1}$ is the identity matrix, and λ_1, λ_2, and λ_3 are the principal moments. From Equation (15) we see that the important quantities are the differences between the principal moments, $(\lambda_3 - \lambda_1)$, $(\lambda_3 - \lambda_2)$ and $(\lambda_2 - \lambda_1)$. These quantities may be rewritten in terms of degree-two real sperical harmonics (e.g. Dahlen et al. 1999). The relevant (fully normalized) harmonics are, in Cartesian coordinates:

$$\begin{aligned} Y_{20} &= \frac{1}{4}\sqrt{\frac{5}{\pi}} \frac{2z^2 - x^2 - y^2}{r^2} \\ Y_{22} &= \frac{1}{4}\sqrt{\frac{15}{\pi}} \frac{x^2 - y^2}{r^2}. \end{aligned} \tag{A.3}$$

Solving for $(\lambda_i - \lambda_j)$ in terms of these harmonics, we find

$$
\begin{aligned}
(\lambda_2 - \lambda_1) &= 4\sqrt{\frac{\pi}{15}} \int_V \rho r^2 Y_{22}\, dV \\
(\lambda_3 - \lambda_1) &= 2\sqrt{\frac{\pi}{15}} \int_V \rho r^2 \left(Y_{22} - \sqrt{3} Y_{20}\right) dV \\
(\lambda_3 - \lambda_2) &= -2\sqrt{\frac{\pi}{15}} \int_V \rho r^2 \left(Y_{22} + \sqrt{3} Y_{20}\right) dV.
\end{aligned}
\tag{A.4}
$$

Up to the normalization constants, these expressions are idential to multipole expansions, picking out the degree-two part of the density field laterally, and low-order polynomials radially. When density is a function of temperature, we can insert the equation of state, Equation (22), into Equation (A.4) and integrate over a reference spherical volume V_S. This allows us to drop the terms which integrate to zero due to the orthogonality of spherical harmonics, and we are left with:

$$
\begin{aligned}
(\lambda_2 - \lambda_1) &= -4\sqrt{\frac{\pi}{15}} \alpha \rho_0 \int_{V_S} T r^2 Y_{22}\, dV \\
(\lambda_3 - \lambda_1) &= -2\sqrt{\frac{\pi}{15}} \alpha \rho_0 \int_{V_S} T r^2 \left(Y_{22} - \sqrt{3} Y_{20}\right) dV \\
(\lambda_3 - \lambda_2) &= 2\sqrt{\frac{\pi}{15}} \alpha \rho_0 \int_{V_S} T r^2 \left(Y_{22} + \sqrt{3} Y_{20}\right) dV.
\end{aligned}
\tag{A.5}
$$

We normalize the differences in eigenvalues by the reference moment I_0:

$$
I_0 = \frac{2}{3} \int_{V_S} \rho_0 r^2\, dV. \tag{A.6}
$$

Dividing Equation (A.5) by I_0 and nodimensionalizing the integrals results in a factor of $\Gamma = \alpha \Delta T$ and a normalized set of degree-two coefficients for the temperature field, which we abbreviate as $T_{\text{degree-two}}$:

$$
\Lambda_{ij} \sim \Gamma T_{\text{degree-two}}. \tag{A.7}
$$

Response to referee

Ian Rose and Bruce Buffett

We thank Yanick Ricard for his thoughtful review. In addition to several smaller suggestions and corrections, his review centers on our treatment of the reference frames relevant to the scaling of true polar wander (TPW). We append his review to this response for convenience. We broadly agree with his criticism, and have substantially reworked our discussion of reference frames to address it. Several of the key equations have been corrected, and we have changed some of the notation for clarity, but the overall conclusions of the manuscript are unchanged.

In particular, we have done the following to clarify and correct the treatment of reference frames:

1. We have added a section (Section 2.2) which makes the differences between reference frames explict. We identify three frames which are important to the problem: (1) the inertial, nonrotating frame, (2) A body-fixed geographic frame, rotating with respect to the inertial frame with relative rotation vector $\mathbf{\Omega}$, and (3) The frame described by the principal axes of the convective moment of inertia $\mathbf{E}$, which we call the $\mathbf{E}$-frame. This frame rotates slowly with respect to the body-fixed frame with rotation vector $\mathbf{\Psi}$.

2. We have added a new figure (Figure 1) which illustrates the different reference frames.

3. We have changed the discussion in Section 2.5 to clarify that the rate of TPW is measured in the body-fixed frame. The rate of TPW we denote by $\dot{\Theta}$. The physics describing the magnitude of $\dot{\Theta}$ are more naturally expressed in the $\mathbf{E}$-frame, with colatitude θ and longitude ϕ. For much of the discussion we make the simplifying assumption that $\phi = 0$. If the $\mathbf{E}$-frame is not rotating with respect to the body fixed frame ($\mathbf{\Psi} = 0$) then $\dot{\Theta} = \dot{\theta}$.

4. We have updated the discussion of the time evolution of the mismatch angle θ (Section 4.2) in light of the changes to the reference frames. The characteristic size of θ is set by the competition of its decay via TPW and

its growth via $\mathbf{\Psi}$. This is reflected in Equations (43) and (44). Our scaling furnishes estimates of the sizes of these two processes.

Besides the discussion of reference frames, we have addressed the following other issues raised in the review:

- We have added the clarifying intermediate step in Equation (7).
- We have added Equation (21) on the source of the gravitational field.
- We have changed the notation of the ratio of centrifugal to gravitational forces from the fluid-dynamics-inspired "Froude number" to the symobl m more commonly used in geodesy.
- We have clarified discussion of transforming the linear momentum equation to the angular momentum equation (Equations (25)-(29)). The review criticized this transformation as not very useful. While we agree that these equations are not particularly easy to evaluate in practice, they do serve two useful purposes for our scaling: First, they establish the overall consistency between the approximations made for the linear momentum equation (Section 3) and those made for the angular momentum equation (Section 2). Second, Equations (23)-(29) demonstrate the origin of the nondimensionalization that we use for our scaling. In particular, Equations (28)-(29) shows the origin of $\alpha\Delta T$ as an independent nondimensional number.
- We have added additional note on the effect of dynamic compensation on the value of $(1 + k_f^L)$
- The review suggested that stirring and mixing can populate lengthscales smaller than d in the convecting system, where d is the injection lengthscale, roughly set by the thickness of the boundary layers. While mixing can do this, we argue that those lengthscales are quickly homogenized by thermal diffusion, whereas thermal anomalies at larger lengthscales persist for a much longer time.

REVIEW

Y RICARD

This is a very interesting paper that tries to estimate the TPW rate of a convecting body as a function of the Ra number. This has never been done and I hope to see it published eventually. However in its present form, the paper is not acceptable. As far as I understand, 3 angles enter the problem: the angle between geography (say the no-net rotation plate tectonic frame or the hotspot frame) and the rotation axis (whose variation is the TPW), the angle between geography and the inertia principal axis, and θ the angle between rotation and main inertial axis. The authors are confusing these three quantities. I suggest to encourage a resubmission.

I refer to page and lines as x.y.

2.11 ineratia/inertia

3.40 This expression was in fact published first in Spada et al., Nature, 1992.

4.20 Maybe add that by definition for constant rotation, around z, (6) implies

$$J_{zz} = C = (2/3)(ka^5)/(3G)\omega^2$$

and

$$J_{xx} = J_{yy} = A = -(1/3)(ka^5)/(3G)\omega^2$$

hence (7)

5 Here I disagree for various aspects!

First I compute $E.\omega - (\omega.E.\omega)\omega$ in the inertia frame with vectors k_1, k_2, k_3 where $\omega = \sin(\theta)\cos(\phi)k_1 + \sin(\theta)\sin(\phi)k_2 + \cos(\theta)k_3$ and I get

$$\begin{bmatrix} \left(\lambda_1 - (\sin(\theta))^2 (\cos(\phi))^2 \lambda_1 - (\sin(\theta))^2 (\sin(\phi))^2 \lambda_2 - (\cos(\theta))^2 \lambda_3\right) \sin(\theta)\cos(\phi) \\ \left(\lambda_2 - (\sin(\theta))^2 (\cos(\phi))^2 \lambda_1 - (\sin(\theta))^2 (\sin(\phi))^2 \lambda_2 - (\cos(\theta))^2 \lambda_3\right) \sin(\theta)\sin(\phi) \\ \left(1/2\ (\lambda_3 - \lambda_1)(\cos(\phi))^2 + 1/2\ (\lambda_3 - \lambda_2)(\sin(\phi))^2\right) \sin(2\theta)\sin(\theta) \end{bmatrix}$$

1) This expression is in the inertia frame with vectors k_1, k_2, k_3. Then, if I try to understand what you did, you have probably written $\dot{\omega} = (\cos(\theta)\cos(\phi)\dot{\theta} - \sin(\theta)\sin(\phi)\dot{\phi})k_1 + (\cos(\theta)\sin(\phi)\dot{\theta} + \sin(\theta)\cos(\phi)\dot{\phi})k_2 - \sin(\theta)\dot{\theta}k_3$ *assuming that the k_i are not time dependent (which is obviously wrong!)*. So, identifying the k_3 components you got

$$\dot{\theta} = -\frac{1}{2}\frac{1}{(C-A)T_1}\left((\lambda_3 - \lambda_1)(\cos(\phi))^2 + (\lambda_3 - \lambda_2)(\sin(\phi))^2\right)\sin(2\theta)$$

which is your first equation (13) where you have missed a 1/2 (I can also get your second equation also missing a 1/2).

2) However, *you just cannot forget to derivate the k_i*. Assuming for now that everything occurs along $\phi = 0$ and that the position of the inertia principal axis moves with angular velocity $\dot{\gamma} k_2$, around the y axis then

$$dk_1/dt = \dot{\gamma} k_2 \times k_1 = -\dot{\gamma} k_3$$

So that the correct k_3 component is now

$$\dot{\theta} + \dot{\gamma} = -\frac{1}{2}\frac{1}{(C-A)T_1}(\lambda_3 - \lambda_1)\sin(2\,\theta)$$

Or working with the absolute coordinates $\theta' = \theta + \gamma$

$$\dot{\theta}' = -\frac{1}{2}\frac{1}{(C-A)T_1}(\lambda_3 - \lambda_1)\sin\left(2\,(\theta' - \gamma)\right)$$

So we get the usual "donkey after the carrot" behavior where θ' wants to coincide with γ but γ lives is own life...

3) What really TPW is, is an absolute motion of the geography with respect to ω (or symmetrically the absolute motion of ω), it is not the relative motion of ω with respect to γ (i.e., it is θ' not θ that matters). Paleomagneticiens cannot measure the angle with respect to the inertia frame.

4) If I try to do the math correctly (but so rapidly that you really have to check what I write although the general procedure should be fine), I start with an absolute frame (E_1, E_2, E_3) and I get the inertia frame (k_1, k_2, k_3) by the classical three Euler rotations: α around E_3 to obtain the frame (i_1, i_2, E_3), then β around i_1 to obtain the frame (i_1, j_2, j_3), then γ around j_3 to reach (k_1, k_2, k_3) (see e.g., wiki page on Euler angles). The rotation of the inertia frame is

$$O = \dot{\alpha} E_3 + \dot{\beta} i_1 + \dot{\gamma} k_3 = \dot{\alpha} E_3 + \dot{\beta}(\cos(\alpha) E_1 + \sin(\alpha) E_2) + \dot{\gamma} k_3$$

so that

$$dk_1/dt = O \times k_1 = \dot{\alpha} E_3 \times k_1 + \dot{\beta}(\cos(\alpha) E_1 \times k_1 + \sin(\alpha) E_2 \times k_1) + \dot{\gamma} k_3 \times k_1$$

and (assuming that I did not screw up in expressing the E_i as a function of the k_i)

$$dk_1/dt = (\dot{\gamma} + \dot{\alpha}\cos(\beta))k_2 + (\dot{\beta}\sin(\gamma) - \dot{\alpha}\cos(\gamma)\sin(\beta))k_3$$

(I guess these kind of expressions should be found in textbooks about solid rotation) ... The same thing should be done for dk_2/dt and dk_3/dt, then we can redo correctly your (13) and get two equations for $\dot{\theta}$ and $\dot{\phi}$ that should also include the three Euler angle time derivatives. The TPW can then be computed in the absolute frame (E_1, E_2, E_3).

6-35 You should add

$$g = -\nabla V$$

and

$$\nabla^2 V = 4\pi G \rho$$

or remove the centrifugal force from (16), and add

$$\nabla^2 V = 4\pi G \rho - 2\Omega^2$$

It is important that the reader realizes that g is not independent of the rotational dynamic and the internal masses. And as g "includes" classically rotation, my second suggestion might be better.

6-58 Although with my physical background I can accept the "Froude" number, it seems to me that since Clairaut (https://en.wikipedia.org/wiki/Clairaut_theorem), all the geodesists (see Lambeck, Nakiboglu 82, Chambat et al, 2010...) use $m = \omega^2 R^3/GM$. Later, you call Γ something usually named in the convection literature ϵ (Γ is often a Gruneisen parameter).

7-42 You should write or explain how the first terms can be transformed in surface integrals and cancel...

equation 24-25 are not really useful. They look nice but really they are problematic. First ΔV cannot be properly define: when the Earth is above its hydrostatic figure, the ΔV is a real volume, but what is it when the Earth is below its hydrostatic figure? ie, when ΔV is "negative"? Furthermore in (4) E includes the surface deflections due to the convection in a non rotating Earth, what the RHS of (25) does not include it. So the mathematical background of (25) and its connection with (4) are weak.

10-40 I do not want to be finicky but k_f^L is -1 near the surface and the CMB so that $1+k$ is rather 1/2 or below... (at least for a uniform viscosity, you can analytically compute $< 1 + k >$ average in depth, see Hager, Forte or myself, somewhere).

11 although your scaling looks good, the reasoning is strange. d is the lithosphere thickness, so heterogeneities are injected at d and diffusion and stirring should populate the nodes with wavelengths smaller than d. But in fact you consider that only wavelengths larger than d exist.

13 As I disagree with your basic equation I cannot follow. The TPW is not $\dot{\theta}$ (an angle relative to main inertia) but the absolute velocity of ω. The rate $\dot{\theta}$ and rate at which the inertia main axis position moves (what I named O above, or the Euler rate $\dot{\alpha}$, $\dot{\beta}$, $\dot{\gamma}$) are not the same thing.

I stop my reading around p13. I am sorry to be negative but I think the authors have a nice problem in hand to solve. But just now, I cannot agree with their physics.